2007

Effects of local Joule heating on the reduction of contact resistance between carbon nanotubes and metal electrodes

Lifeng Dong

Steven Youkey

Jocelyn Bush

Jun Jiao

V M. Dubin

See next page for additional authors

Recommended Citation

Dong, Lifeng, Steven Youkey, Jocelyn Bush, Jun Jiao, Valery M. Dubin, and Ramanan V. Chebiam. "Effects of local Joule heating on the reduction of contact resistance between carbon nanotubes and metal electrodes." Journal of applied physics 101, no. 2 (2007): 024320.

Effects of local Joule heating on the reduction of contact resistance between carbon nanotubes and metal electrodes

Lifeng Dong,[a] Steven Youkey, Jocelyn Bush, and Jun Jiao[b]
Department of Physics, Portland State University, Portland, Oregon 97207-0751

Valery M. Dubin and Ramanan V. Chebiam
Components Research, Intel Corporation, Hillsboro, Oregon 97124

(Received 31 May 2006; accepted 16 November 2006; published online 24 January 2007)

We report here a practical application of known local Joule heating processes to reduce the contact resistance between carbon nanotubes and metallic electrical contacts. The results presented in this study were obtained from a series of systematic Joule heating experiments on 289 single-walled carbon nanotubes (SWCNTs) and 107 multiwalled carbon nanotubes (MWCNTs). Our experimental results demonstrate that the Joule heating process decreases the contact resistances of SWCNTs and MWCNTs to 70.4% and 77.9% of their initial resistances, respectively. The *I-V* characteristics of metallic nanotubes become more linear and eventually become independent of the gate voltages (V_{gs}). For semiconducting nanotubes, the contact resistance has a similar decreasing tendency but the dependency of source-drain current (I_{ds}) on V_{gs} does not change with the Joule heating process. This suggests that the reduction of the contact resistance and the decrease of the transport potential barrier are largely attributed to the thermal-energy-induced desorption of adsorbates such as water and oxygen molecules from the nanotube surface and the interface region, as well as thermal-energy-enhanced bonding between the nanotubes and electrode surfaces. In comparison to several other methods including rapid thermal annealing, e-beam lithography patterning of the top metal layer, and focused ion beam induced metal deposition of the top layer, the Joule heating process not only effectively reduces the contact resistance but also simultaneously measures the resistance and monitors the change in the transport potential barrier at the interface region. © *2007 American Institute of Physics*. [DOI: 10.1063/1.2430769]

I. INTRODUCTION

Since the demonstration of carbon nanotube (CNT) field effect transistors (FET) in 1998, intensive efforts have been made to achieve the fabrication of CNT-based devices (such as FETs and electrical interconnects) followed by extensive studies of their electronic properties.[1,2] In particular, CNTs' unique ballistic transport characteristics and high carrier mobility in the diffusive region have attracted a great deal of attention.[3–7] However, two well-recognized barriers prevent the realization of the full potential of CNT-based devices, despite their desirable electronic properties: (1) a lack of an effective method to separate bundled CNTs into individuals and to place them at designated locations and (2) the fabricated devices usually demonstrate much higher resistances than the quantum limited value for a one-dimensional system ($h/4e^2 \sim 6.25$ kΩ). In general, the reported contact resistances between the CNTs and metallic electrical contacts range from 10^4 to 10^9 Ω.[8–14] Such high resistance severely prevents the CNT-based devices from reaching the intrinsic electronic properties of CNTs. The formation of a good contact with low resistance between the CNTs and metallic microelectrodes is critical to the application of CNTs in nanoscale electronic devices. Although various attempts have been made by a number of groups, an effective technique for reducing the contact resistance of CNT devices has yet to be developed. For example, by exposing the CNT contact area to a focused electron beam, the contact resistance can be decreased by several orders of magnitude.[13] However, the irradiation of the electron beam could deform and even burn out the nanotubes. Lee *et al.* developed a method for reducing contact resistance by rapid thermal annealing (RTA) CNT devices at 600–800 °C for 30 s. In this case, the entire substrate including CNTs, patterned metallic electrodes, and other device components underwent the high-temperature process (600–800 °C).[14] Such high temperature will severely limit the selection of materials that can be used on the substrate. For instance, aluminum (Al) interconnects have a melting point around 660 °C and would thus be deformed or melted during the RTA process.

In an effort to overcome the two main barriers mentioned above, we recently developed an effective floating-potential dielectrophoretic method to purify and disperse CNT bundles and subsequently to align both individual metallic and semiconducting CNTs between two electrical contacts.[15] This development allows us to fabricate a large number of CNT-based devices and to systematically study the contact resistance of the interface region between nanotubes and electrodes. In this study, a total of 396 individual nanotubes [289 single-walled carbon nanotubes (SWCNTs) and 107 multiwalled carbon nanotubes (MWCNTs)] were dielectrophoretically aligned between two electrical contacts,

[a]Present address: Department of Physics, Astronomy, and Materials Science, Missouri State University, Springfield, Missouri 65897.
[b]Author to whom correspondence should be addressed; electronic mail: jiaoj@pdx.edu

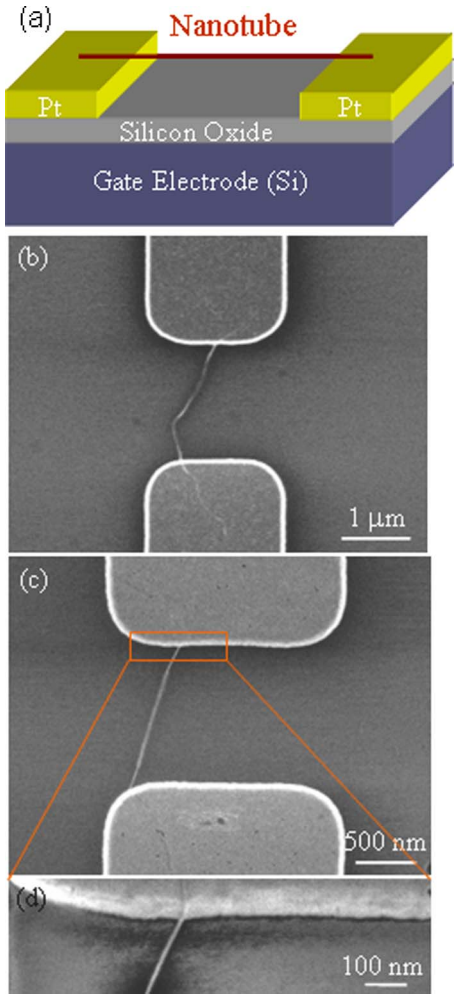

FIG. 1. (a) A schematic diagram of the back-gated nanotube testing structure. (b) SEM image of an individual MWCNT aligned on top of two electrical contacts. (c) SEM image of an individual SWCNT positioned on the surface of two electrodes, which is verified by a high-magnification SEM image (d).

and a local Joule heating process was investigated to enhance the nanotube-electrode contact. Our experimental results demonstrate that the reductions in resistance achieved by the Joule heating process are comparable with those obtained by other techniques such as RTA, and the fabrication of a top metal layer onto aligned nanotubes by electron beam lithography (EBL) and focused ion beam (FIB) induced metal depositions.

II. EXPERIMENT

Figure 1(a) shows a schematic diagram of the CNT device used for this study. Each device contains an aligned nanotube with platinum (Pt) source/drain contacts and a silicon substrate gate contact. The SWCNTs, with a diameter of 1–3 nm and a length of several micrometers, were purchased from BuckyUSA. The MWCNTs with an average diameter of 10 nm and a length ranging from several micrometers to tens of micrometers were synthesized by a thermal chemical vapor deposition (CVD) process in our laboratory.[16,17] Patterned Pt contacts were fabricated on silicon substrates coated with a 1-μm-thick thermal oxide layer for the purpose of determining whether the aligned CNTs were metallic or semiconducting. Prior to the dielectrophoretic alignment, SWCNTs or MWCNTs were dispersed in de-ionized water containing 1 wt % sodium dodecyl sulfate (SDS).[18] After sonication and centrifugation, a drop of nanotube suspension was applied onto a region consisting of several patterned electrodes. An ac electric potential ($1-10\ V_{p-p}$, 50 kHz–10 MHz) was then applied onto two control electrodes for 1 min. The substrates with aligned CNTs were soaked in de-ionized water for 30 min to remove SDS molecules from CNT surfaces by dissolution[19] and then dried with flowing nitrogen gas.

III. RESULTS AND DISCUSSION

A. Floating-potential dielectrophoretic alignment of individual carbon nanotubes

An FEI Sirion field emission scanning electron microscope (SEM) was utilized to characterize the morphology and the orientation of the individual CNTs aligned between two electrodes as well as to map the location of the aligned CNTs. As shown in Figs. 1(b)–1(d), both individual MWCNTs and SWCNTs can be aligned between two electrical contacts by the floating-potential dielectrophoresis process. We observed that bundled nanotubes and a large number of impurities were positioned between the two control electrodes, while individual nanotubes were aligned between two electrodes with floating potentials. This phenomenon can be attributed to the fact that the electric force is proportional to the volume of suspension particles and the gradient of the electric field. The field gradient in the control region is larger than that in the floating-potential regions. Thus, when a drop of nanotube suspension is applied onto a region consisting of two control electrodes (one control electrode was grounded and another control electrode was applied with ac potential) and three or four floating electrodes, bundles of nanotubes, and a large volume of impurities are attracted favorably towards the region between two control electrodes. After filtering most of the nanotube bundles and impurities into the control region, the individual nanotubes remaining in the drop of solution were aligned between two floating electrodes. The detailed alignment mechanism is discussed elsewhere.[15] Furthermore, because of the electrostatic force between the electric-field-induced charges on the electrode surface and an electric-field-induced nanotube dipole, one end of the individual nanotube will be attracted towards the top surface of the electrode. If the nanotube is longer than the gap distance between two electrodes, its other end will sit on top of the opposite electrode.[20] Figures 1(b) and 1(d) show clearly that both ends of an aligned MWCNT and SWCNT are positioned on top of two electrodes, respectively. The contact length between the nanotubes and the electrode surface ranges from several nanometers to hundreds of nanometers, depending on the full length of a CNT in relation to the gap distance between the electrodes. The height profile of atomic force microscopy (AFM) characterization in combination with SEM characterizations is used to determine whether an individual nanotube or a small bundle is aligned between two electrodes.

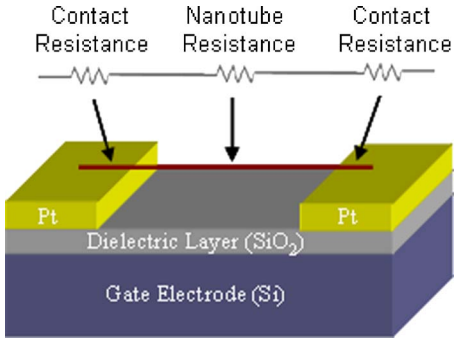

FIG. 2. Illustration of the measured resistance consisting of intrinsic nanotube resistance and contact resistances between aligned nanotube and electrode surfaces.

B. Effects of local Joule heating on the contact resistance of SWCNTs

Following the SEM-mapped CNT positions on the substrate, the electrical contacts aligned with individual CNTs can be accurately located under a probe station (Cascade Microtech Summit MicroChamber). The source-drain current (I_{ds}) through the CNTs as a function of the bias voltage (V_{ds}) and the gate voltage (V_{gs}) was measured at room temperature using standard dc techniques with an Agilent 4156C semiconductor parameter analyzer. Our electrical measurement results show that the resistance of both aligned MWCNTs and SWCNTs vary from 10^4 to 10^8 Ω, falling in the same range as those of nanotube devices fabricated by other methods.[8–14] To understand the origin of contact resistance, Fig. 2 indicates that the measured resistance is the sum of nanotube and contact resistances. Since ballistic transport has been reported on both semiconducting and metallic nanotubes,[3] the measured resistance mainly resulted from contact resistances between nanotubes and metallic contacts. Our calibration measurements also indicate that the resistance between testing microprobes and Pt electrodes is only several ohms. The influence of this resistance on the measured nanotube resistance, therefore, is negligible. Considering that the contact resistance is much larger than the intrinsic resistance of aligned nanotubes, we believe that significant Joule heating (electrical power: $P=I^2R=V^2/R$) would mainly occur at the interface region between the nanotube and electrode surface while electrical carriers pass through the nanotube channel. For instance, when a 1 μA electric current I is applied, the power P applied onto the interface will range from 0.01 to 100 μW corresponding to a contact resistance of 10^4–10^8 Ω. This power is high enough to anneal the nanoscale interface region, and even to burn out nanotubes. This is verified by our experimental results: when a constant voltage (1–3 V) is applied between two ends of

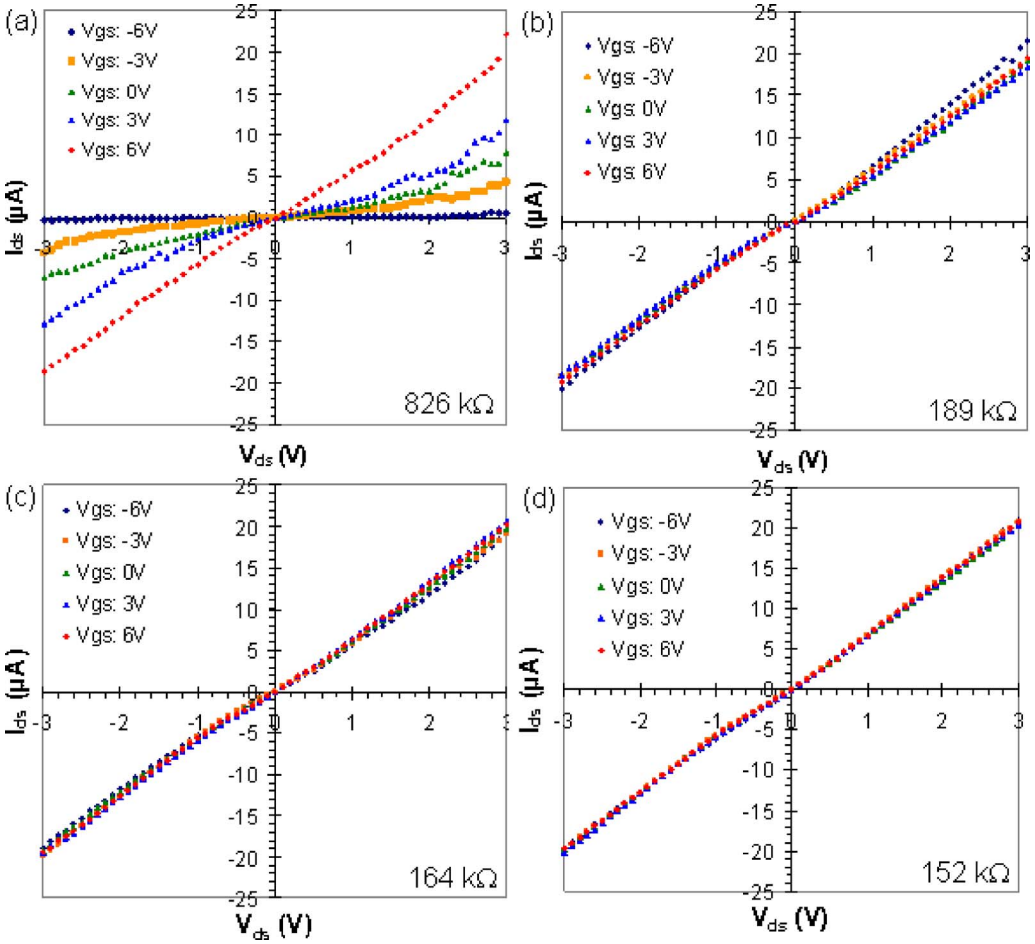

FIG. 3. *I-V* behaviors of an individual SWCNT after different times of Joule heating process: (a) initial status without Joule heating process, (b) after one time of Joule heating, (c) after two times of Joule heating, and (d) after three times of Joule heating.

the aligned nanotubes for 30 or 60 s, an infinite resistance was observed indicating burn-out of the nanotubes. To avoid the accumulation of high heat at the interface region, sweeping voltages were used to provide Joule heating at the interface region instead of a constant voltage or a constant current. As shown in Fig. 3(a), the initial *I-V* curve of an aligned SWCNT behaves like a semiconducting nanotube as I_{ds} currents depend on V_{gs} voltages. The measured resistance at V_{gs}=0 V is about 826 kΩ. During the electrical measurement, V_{gs} was stepped from −6 to 6 V with a step size of 1 V interval, and V_{ds} was swept from −3 to 3 V with a sweeping interval of 0.1 V. It takes 6.5 s to conduct the process of the electrical measurement. That is, the duration time of each sweeping V_{ds} is only about 0.008 s. Since Joule heating occurs at the interface region during electrical measurement, both the physical and chemical properties of the interface region could be altered. Consequently, the resistance was measured again using the same process. The advantages of this sweeping process are that it not only measures the resistance and provides local Joule heating at the interface region but it also tests whether I_{ds} depends on V_{gs} to provide more information about the transport potential barrier at the interface region. As shown in Figs. 3(a) and 3(b), after the sweeping process, the measured resistance was dramatically decreased from 826 to 189 kΩ and the I_{ds} is independent of

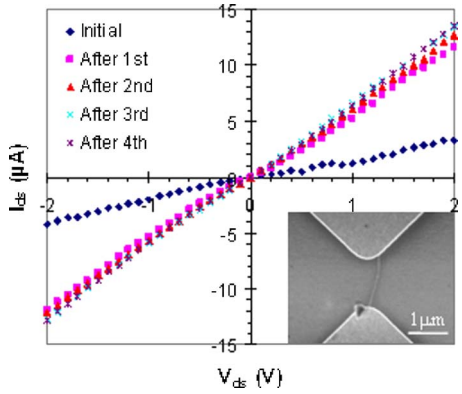

FIG. 4. Comparative *I-V* curves clearly indicate Joule heating process can decrease the barrier to carrier transport. After the Joule heating process, the *I-V* curve displays linear characteristics (inset: SEM image of the SWCNT).

V_{gs}. Two more sweeping processes were then carried out as plotted in Figs. 3(c) and 3(d). The results show that the measured resistance was further decreased to 164 and 152 kΩ after the second and third Joule heating processes. The decrease in magnitude, however, was not as significant as that of the first sweeping process. For a comparison, I_{ds} vs V_{ds} curves at V_{gs}=0 V after different times of Joule heating or sweeping processes are plotted in Fig. 4. It clearly shows that

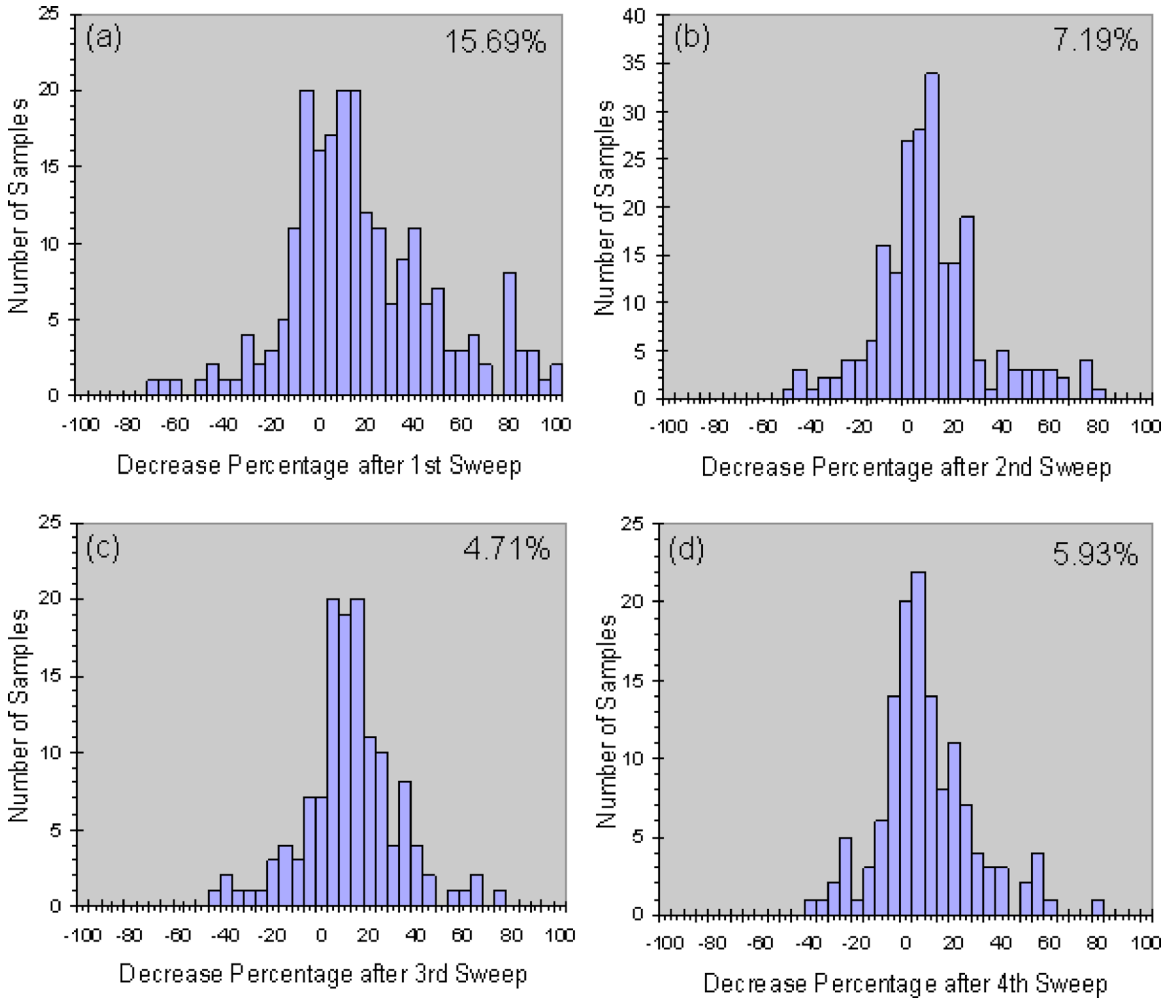

FIG. 5. Histograms of decrease percentage of SWCNT contact resistance after (a) first sweep, (b) second sweep, (c) third sweep, and (d) fourth sweep.

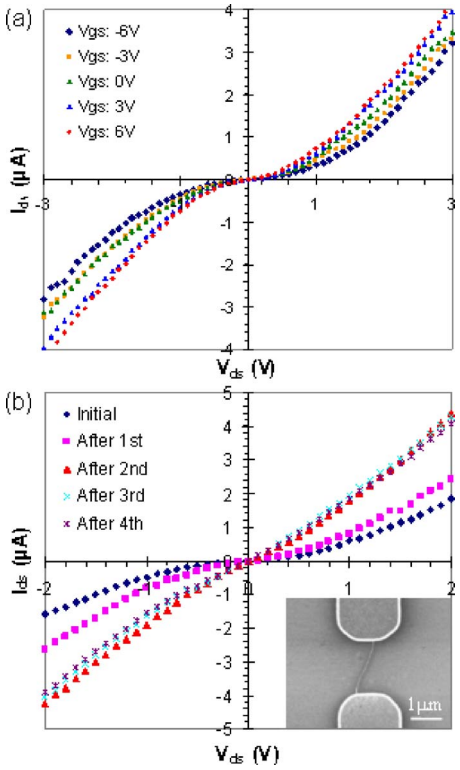

FIG. 6. *I-V* curves of an individual MWCNT became linear after two times of Joule heating process (inset: SEM image of the MWCNT).

the first sweeping process dramatically decreases the contact resistance. Also the *I-V* curve becomes more linear than the initial curve without applying the sweeping process. The final results suggest that the aligned SWCNT in Fig. 3 is metallic rather than semiconducting, although its initial *I-V* characteristics in Fig. 3(a) behave like a semiconductor. We ran similar experiments for a large number of individually aligned CNTs. There were 26 SWCNTs, however, showing unchanged semiconducting *I-V* characteristics. After several sweeping processes, the contact resistance of these 26 SWCNTs had a similar decreasing tendency, but the dependency of I_{ds} on V_{gs} did not change with respect to the sweeping process. Our plausible explanations for these experimental results are as follows. (1) Joule heating occurs locally at the interface region and generates a certain degree of annealing to improve the contact. (2) The thermal energy generated by the local Joule heating causes the release of surface adsorbates, such as water and oxygen molecules, absorbed in the interface region and results in the variation of the conductivity of the nanotube-based devices (metallic versus semiconducting). (3) The annealing process may cause migration of metal atoms from the contact electrodes to the surface of nanotubes. These atoms can, in effect, shield the gate electric fields and therefore significantly reduce the gate dependence.

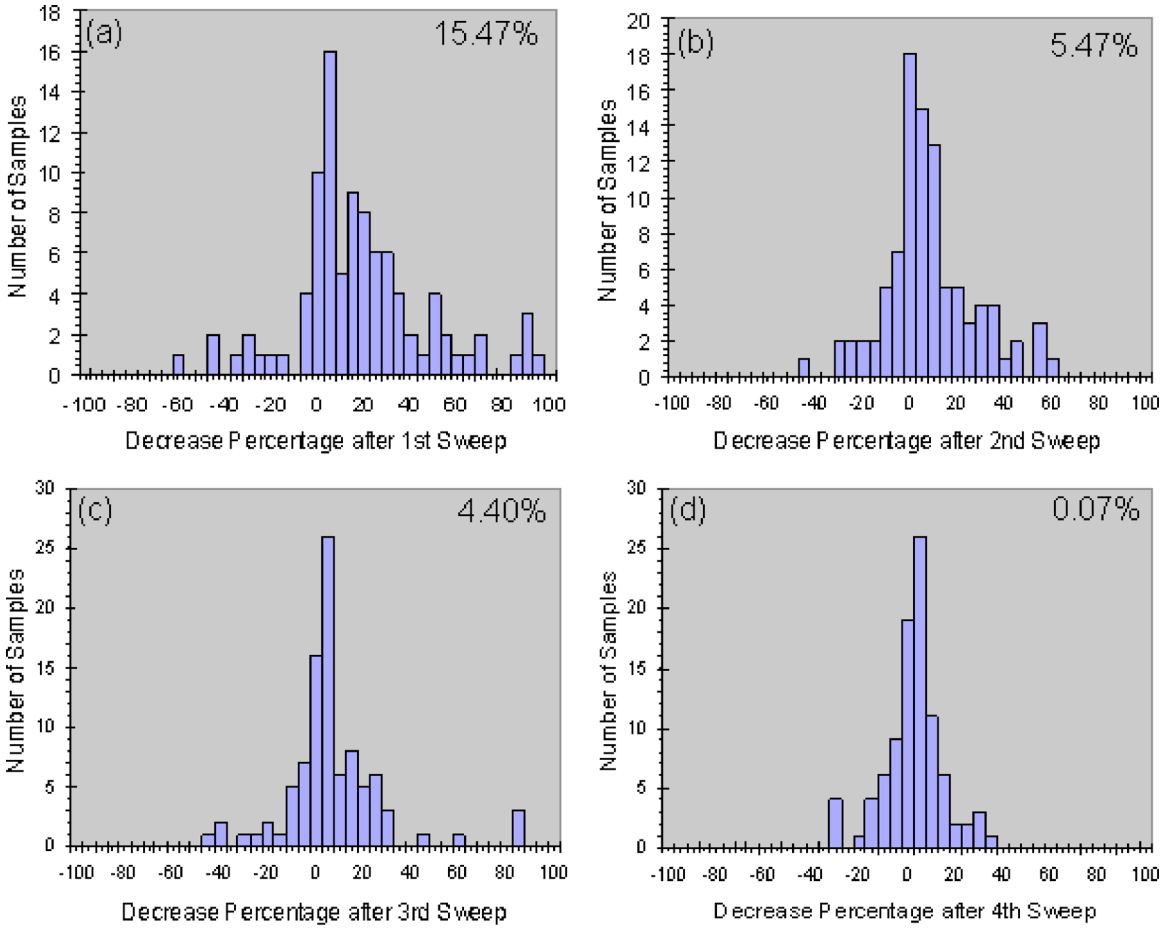

FIG. 7. Histograms of decrease percentage of MWCNT contact resistance after (a) first sweep, (b) second sweep, (c) third sweep, and (d) fourth sweep.

TABLE I. Decrease percentages of contact resistances after first, second, third, and fourth Joule heating processes.

	Sample number	Diameter (nm)	After first sweep (%)	After second sweep (%)	After third sweep (%)	After fourth sweep (%)	Total (%)
SWCNTs	289	1–3	15.69	7.19	4.71	5.93	29.57
MWCNTs	107	4–20	15.47	5.47	4.40	0.07	22.08

In order to systematically evaluate the effectiveness of the local Joule heating process on the reduction of contact resistances, the same sweeping processes were applied five times on each of 289 individual SWCNTs. We employed the sweeping process five times because there is much less reduction at the contact resistance after the fourth sweeping process. As demonstrated by the broad distribution of contact resistances ranging from 10^4 to 10^8 Ω, there are different complex interfaces formed between different SWCNTs and the Pt electrode surface. Thus, we observed that local Joule heating results in varying levels of contact resistance reduction for different nanotube-metal interfaces. Some contact resistances can be decreased by several orders of magnitude after the first Joule heating process. However, we also observed some cases with increased contact resistances. This suggests that the Joule heating process may occasionally cause CNTs to separate from the electrode surface, resulting in an increase of the contact resistance. Overall, Joule heating tends to decrease contact resistance, although the decrease percentage after each sweeping process differs. As summarized in Fig. 5, the average decrease percentages after the first, second, third, and fourth sweepings are 15.69%, 7.19%, 4.19%, and 5.93%, respectively. Therefore, after applying the Joule heating process five times for each sample, the contact resistance of an individual SWCNT can be decreased to 70.43% of the initial measured resistance. Our study also suggests that the reduction of contact resistance caused by Joule heating is irreversible. This was demonstrated by measuring the same samples after 3 months of initial measurements with no observable changes in the contact resistance.

C. Effects of local Joule heating on the contact resistance of MWCNTs

In order to study effects of the Joule heating process on the reduction of contact resistance in nanotubes of different diameters, we also applied the same sweeping process to 109 individual MWCNTs. The diameters of SWCNTs and MWCNTs are in the range of 1–3 and 5–20 nm, respectively. In comparison to SWCNTs, MWCNTs demonstrated similar decreasing behavior caused by the local Joule heating process (Fig. 6). After two sweeping processes, I_{ds}-V_{ds} curves become more linear, indicating that the Joule heating process enhances the bonding between aligned MWCNT and electrode surfaces, thus decreasing the transport potential barrier. However, the magnitude of decrease of MWCNT contact resistances is less than those of SWCNTs (Fig. 7 and Table I). The average decrease percentages after the first, second, third, and fourth sweeping processes are 15.47%, 5.47%, 4.40%, and 0.07%, respectively. Therefore, the contact resistance of MWCNTs can be decreased to about 77.92% of the initial resistance after five repetitions of the Joule heating process. These results indicate that the decreased contact resistances caused by the Joule heating process are related to nanotube structures and interface area. With the same amount of heat applied onto the interface region, the heat density of MWCNTs is lower than that of SWCNTs. This is because MWCNTs have a larger diameter and therefore, a larger interface area between MWCNTs and electrode surface.

D. Comparison of local Joule heating with other methods

Our study also demonstrates that the effectiveness of the Joule heating process for the reduction of contact resistances is comparable to those of other techniques, such as RTA and a top Pt layer deposited onto both ends of aligned nanotubes by EBL or FIB (Table II). However, RTA and FIB deposition caused some nanotubes to burn out. After the deposition of a Pt top layer by EBL, the contact resistance can be decreased by 47.2%. The decrease percentage is higher than that achieved by the Joule heating process. This suggests that it is possible to combine both Joule heating and the EBL process to eventually minimize the contact resistances of CNT-based devices.

IV. CONCLUSIONS

In summary, our experimental results obtained from 396 nanotube samples clearly demonstrate that the local Joule heating process is a simple and reliable technique for electrical measurements and the reduction of contact resistances. This is because it not only measures the resistance of nanotube-based devices and tests whether V_{ds} depends on V_{gs} to provide the information about transport potential barrier but it also locally anneals the interface region between nano-

TABLE II. A comparison of decrease percentages of contact resistances after different processes.

Process		Number of samples	Decrease percentage (%)	Number of damaged nanotubes
RTA annealing at 450 °C for 30 s		42	20.4	9
Top metallic Pt layer deposition	EBL	15	47.2	0
	FIB	52	26.4	11
Local Joule heating after five sweeps	SWCNTs	289	29.6	0
	MWCNTs	107	22.1	0

tube and electrode surfaces to reduce its contact resistance. The mechanism of this reduction is based on the fact that the Joule heating process can desorb molecules absorbed in the interface region and improve the bonding between the nanotube and electrode surfaces. It is possible that a certain amount of Joule heating may cause the migration of metal atoms from the contacts to the surface of nanotubes and result in the shielding of the gate electric fields and reduce the gate dependence of the CNT device. Our study also shows that the reduction of contact resistance is related to nanotube structures. The decrease percentages of contact resistances of SWCNTs and MWCNTs are 29.6% and 22.1%, respectively. Compared with MWCNTs, the reduction percentage of contact resistances of SWCNTs is higher, likely due to their smaller interface regions with electrode surfaces. The next step to improve the effectiveness of the local Joule heating process will be to optimize aspects of the sweeping parameters, such as magnitude and duration time of sweeping electric potential or current. The combination of Joule heating process and the EBL process will also be investigated.

ACKNOWLEDGMENTS

This research was financially supported by the Intel Corp. and the National Science Foundation (DMR-220926). The authors would like to thank Jennifer Lo, Hector Oporta, Vachara Chirayos, and Devon McClain for their help in some of the experiments.

[1]S. Tans, A. Verschueren, and C. Dekker, Nature (London) **393**, 49 (1998).
[2]R. Martel, T. Schmidt, H. R. Shea, T. Hertel, and Ph. Avouris, Appl. Phys. Lett. **73**, 2447 (1998).
[3]A. Javey, J. Guo, Q. Wang, M. Lundstrom, and H. J. Dai, Nature (London) **424**, 654 (2003).
[4]S. Frank, S. P. Poncharal, Z. L. Wang, and W. A. de Heer, Science **280**, 1744 (1998).
[5]C. Berger, Y. Yi, Z. L. Wang, and W. A. de Heer, Appl. Phys. A: Mater. Sci. Process. **74**, 363 (2002).
[6]M. Bockrath, D. H. Cobden, J. Lu, A. G. Rinzler, R. E. Smalley, L. Balents, and P. L. McEuen, Nature (London) **397**, 598 (1999).
[7]M. Ouyang, J. L. Huang, and C. M. Lieber, Acc. Chem. Res. **35**, 1018 (2002).
[8]Z. H. Chen, J. Appenzeller, J. Knoch, Y. M. Lin, and Ph. Avouris, Nano Lett. **5**, 1497 (2005).
[9]M. Liebau, E. Unger, G. S. Duesberg, A. P. Graham, R. Seidel, F. Kreupl, and W. Hoenlein, Appl. Phys. A: Mater. Sci. Process. **77**, 731 (2003).
[10]S. Heinze, J. Tersoff, R. Martel, V. Derycke, J. Appenzeller, and Ph. Avouris, Phys. Rev. Lett. **89**, 106801 (2002).
[11]J. Kong, C. Zhou, A. Morpurgo, H. T. Soh, C. F. Quate, C. Marcus, and H. J. Dai, Appl. Phys. A: Mater. Sci. Process. **69**, 305 (1999).
[12]A. Bachtold, M. Henny, C. Terrier, C. Strunk, and C. Schönenberger, Appl. Phys. Lett. **73**, 274 (1998).
[13]H. Maki, M. Suzuki, and K. Ishibashi, Jpn. J. Appl. Phys., Part 1 **43**, 2027 (2004).
[14]J. O. Lee, C. Park, J. J. Kim, J. H. Kim, J. W. Park, and K. H. Yoo, J. Phys. D **33**, 1953 (2000).
[15]L. F. Dong *et al.*, J. Phys. Chem. B **109**, 13148 (2005).
[16]L. F. Dong, J. Jiao, S. Foxley, C. L. Mosher, and D. W. Tuggle, J. Nanosci. Nanotechnol. **2**, 155 (2002).
[17]L. F. Dong, J. Jiao, C. C. Pan, and D. W. Tuggle, Appl. Phys. A: Mater. Sci. Process. **78**, 9 (2004).
[18]M. J. O'Connell *et al.*, Science **297**, 593 (2002).
[19]C. Richard, F. Balavoine, P. Schultz, T. W. Ebbesen, and C. Mioskowski, Science **300**, 775 (2003).
[20]L. F. Dong, J. Bush, V. Chirayos, J. Jiao, Y. Ono, J. F. Conley Jr., and B. D. Ulrich, Nano Lett. **5**, 2112 (2005).